NASA TECHNICAL MEMORANDUM

NASA TM X-3144

NASA TM X-3144

CONTINUOUS-OUTPUT TERMINAL-SHOCK-POSITION SENSOR FOR MIXED-COMPRESSION INLETS EVALUATED IN WIND-TUNNEL TESTS OF YF-12 AIRCRAFT INLET

by Miles O. Dustin, Gary L. Cole, and George H. Neiner

Lewis Research Center
Cleveland, Ohio 44135

NATIONAL AERONAUTICS AND SPACE ADMINISTRATION • WASHINGTON, D. C. • DECEMBER 1974

1. Report No.	2. Government Accession No.	3. Recipient's Catalog No.
NASA TM X-3144		

4. Title and Subtitle	5. Report Date
CONTINUOUS-OUTPUT TERMINAL-SHOCK-POSITION SENSOR FOR MIXED-COMPRESSION INLETS EVALUATED IN WIND-TUNNEL TESTS OF YF-12 AIRCRAFT INLET	December 1974
	6. Performing Organization Code
7. Author(s)	8. Performing Organization Report No.
Miles O. Dustin, Gary L. Cole, and George H. Neiner	E-7808
	10. Work Unit No.
9. Performing Organization Name and Address	766-72
Lewis Research Center National Aeronautics and Space Administration Cleveland, Ohio 44135	11. Contract or Grant No.
	13. Type of Report and Period Covered
12. Sponsoring Agency Name and Address	Technical Memorandum
National Aeronautics and Space Administration Washington, D.C. 20546	14. Sponsoring Agency Code

15. Supplementary Notes

16. Abstract

A new electronic sensor has been built to measure the position of the terminal shock in a supersonic inlet. The sensor uses several static-pressure taps in the inlet wall. The sensor output is continuously proportional to shock position. Previous sensors had discrete output levels that were proportional to shock position. Installed in a YF-12 aircraft flight inlet during wind-tunnel tests, the sensor indicated shock position within ±5 percent of the total distance covered by the static-pressure-tap region. The maximum error caused by an angle-of-attack change of 4° was less than 25 percent. In the region of normal inlet operation, the angle-of-attack error is negligible. Frequency-response tests show the amplitude ratio is constant out to 60 Hz, and decreases to about 50 percent at 100 Hz, with a phase lag of 50°.

17. Key Words (Suggested by Author(s))	18. Distribution Statement
Terminal shock; Shock; Sensor; Shock sensor; Supersonic; Inlet; Intake	Unclassified - unlimited Category 28

19. Security Classif. (of this report)	20. Security Classif. (of this page)	21. No. of Pages	22. Price*
Unclassified	Unclassified	24	$3.25

* For sale by the National Technical Information Service, Springfield, Virginia 22151

CONTINUOUS-OUTPUT TERMINAL-SHOCK-POSITION SENSOR FOR MIXED-COMPRESSION INLETS EVALUATED IN WIND-TUNNEL TESTS OF YF-12 AIRCRAFT INLET

by Miles O. Dustin, Gary L. Cole, and George H. Neiner

Lewis Research Center

SUMMARY

This report describes the design and performance of a sensor that determines the position of the terminal shock in mixed-compression supersonic inlets. The sensor uses the abrupt rise in static pressure across the shock to determine the shock position. The static-pressure profile along the duct wall is measured by high-response pressure transducers connected to closely spaced static-pressure taps.

The sensor is the result of a continuing program to develop shock sensors for supersonic inlets. Other sensors developed under this program have outputs that consist of several levels. The output increases one level when the shock moves upstream over another tap. The number of output levels depends on the number of pressure taps. The sensor described in this report differs from these sensors in that it has a continuous output that is proportional to shock position rather than having discrete output levels.

The sensor was evaluated in a YF-12 aircraft flight inlet in the 10- by 10-Foot Supersonic Wind Tunnel of the NASA Lewis Research Center. Both steady-state and dynamic tests were conducted.

The sensor linearity, determined by static tests, was within ±5 percent of the total distance covered by the static-pressure tap region. The maximum error caused by an angle-of-attack change of 4° was less than 25 percent. A gain change of about 7 percent occurred over the same 4° angle-of-attack change. In the region of normal inlet operation, the angle-of-attack error is negligible.

Frequency-response tests on the sensor show that the amplitude ratio is constant to 60 hertz and decreases to about 50 percent at 100 hertz. The phase lag at 100 hertz was about 50°.

INTRODUCTION

A high-Mach-number supersonic aircraft derives a large portion of its propulsive effort from the inlet (ref. 1). It is, therefore, important to use a mixed-compression inlet and to operate it at maximum performance. In order to achieve high pressure recovery at the engine face with low distortion levels, the inlet must operate with the terminal shock downstream of throat and as close to the throat as possible. If the terminal shock moves further downstream, it will occur at a higher Mach number, and this will result in large pressure losses across the shock. This creates low pressure recovery and high pressure distortion at the compressor face. If the shock moves too close to the throat, an airflow disturbance, caused by either atmospheric turbulence, originating external to the inlet, or a change in engine airflow, can cause the shock to move into the unstable region upstream of the throat and thereby cause the inlet to unstart. A shock position margin is required. The size of the margin depends on the capabilities of the terminal-shock control, the accuracy with which the shock position is known, and the nature of expected disturbances.

Most supersonic inlet control systems use a duct static pressure taken downstream of the terminal shock to infer the shock position. The gain of this measurement is usually nonlinear, and the signal must be biased to compensate for inaccuracies due to operating at off-design Mach numbers, altitudes, angles of attack, and yaw angles. An alternate approach is to measure the shock position directly. References 2 to 7 describe efforts to measure the shock position directly from measurements of several static-pressure taps located in the vicinity of the shock. The output consists of several levels, and it increases or decreases by one level whenever the shock moves upstream or downstream over one of the taps. The number of levels depends on the number of pressure taps. The stepwise nature of the output makes this type of sensor unsuitable, in most cases, for closed-loop shock-position control. For example, if the shock-position controller had integral action, the control system would cause the output to oscillate between two sensor output levels.

This report describes a shock sensor that compares each of several cowl static-pressure levels with a reference pressure (as described in refs. 5 to 7) but has a continuous output that is proportional to shock position rather than having discrete output levels. The continuous-output shock-position sensor was evaluated in a YF-12 aircraft flight inlet in the 10- by 10-Foot Supersonic Wind Tunnel of the NASA Lewis Research Center. A complete description of the inlet, instrumentation, and tunnel installation is given in reference 8. Wind-tunnel studies of the operational YF-12 aircraft inlet control system and of experimental control systems are discussed in references 9 and 10, respectively. A frequency-response evaluation of the inlet is presented in reference 11. The steady-state performance of the inlet is reported in reference 12.

SYMBOLS

M	Mach number
$P_{p,A}$	throat total-pressure probe (see fig. 8)
$P_{s,A}, P_{s,B}, \ldots, P_{s,J}$	static-pressure tap designations (see fig. 8)
r_{cl}	radius of cowl at cowl-lip station (74.62 cm)
t	time, sec
X_{cl}	axial distance of local station from cowl lip, cm
x_s	shock-position-sensor output, cm
Δx	shock displacement, cm
φ	phase angle, deg
ω	frequency, Hz

SENSOR DEVELOPMENT BACKGROUND

The work described in this report is the continuation of the development of the shock sensors described in references 2 to 7. The background information presented in this section will aid the reader in understanding the principles of operation of both the stepwise-output sensors described in references 2 to 7 and the continuous-output sensor.

For inlets with internal compression, the ideal static-pressure profile occurs as shown in figure 1. The minimum supersonic flow Mach number occurs at the inlet throat. Downstream of the throat, the Mach number increases and static pressure decreases as area increases. At the terminal shock, there is a discontinuous rise in pressure. Downstream of the shock, the pressure continues to rise, since the flow is subsonic, and the area continues to increase.

An actual pressure profile is not ideal like the profile shown in figure 1. Figure 2 shows typical cowl-wall static-pressure profiles for a mixed-compression inlet as measured by a series of closely spaced static-pressure taps. Curves for three different shock positions are shown. Each profile was obtained with the location of the leading edge of the shock as noted in the figure. The non-ideal nature of the profiles is due to such things as interactions between the shock and the boundary layer, oblique shock reflections, and a finite shock train length. Although the pressure rise across the shock is not sharply discontinuous as in the ideal case, there is a large pressure gradient in the vicinity of the shock. This gradient may be used for determining shock position.

The most practical of the sensors evaluated in references 2 to 7 compared each wall static-pressure tap with a reference pressure. A schematic representation of a shock sensor similar to the electronic sensor used in reference 7 is shown in figure 3. Only five cowl static-pressure taps are shown. More may be used if greater accuracy or wider range of shock position is desired. Each cowl static pressure is compared to a reference pressure, in this case, a fraction of the throat total pressure. If the cowl static pressure is greater than the reference pressure, the comparator output for that tap will be "on." The outputs of the individual comparators are summed in the output summing amplifier to provide a single output signal. The sensor output then consists of a series of levels. The output level depends on the number of static-pressure taps that exceed the reference pressure. The resulting output is not continuous with shock position, but is stepwise in nature, increasing in level when the shock moves upstream. If 10 taps are used, the sensor will have 11 output levels.

The sensor shown in figure 3 has an additional feature not included in the sensor used in reference 7. Each reference voltage can be adjusted to a different level by means of the individual, voltage-dividing, reference potentiometers. This allows the reference voltage for each tap to be set a small amount greater than the supersonic value corresponding to that tap. The principle of operation of the sensor can be illustrated by figure 4. The supersonic static-pressure profile is the heavy line. For the purpose of this illustration, each reference-pressure voltage was set 0.025 pressure-ratio units greater than the supersonic pressure profile. This margin will depend on things such as noise in the static-tap pressures and variation in the supersonic pressure profile due to the angle of attack of the inlet. For the profile designated by the triangular data-point symbols in figure 4, the sensor would have all outputs for taps $P_{s,E}$ to $P_{s,J}$ turned on, since their pressure values are greater than the reference pressure for this profile.

Typical output signals for the stepwise-output-type sensors are shown in figure 5. These oscilloscope traces were taken from reference 7. These output traces are from two sensors using the same logic. One sensor implemented this logic by electronic means, and the other by fluidic means. These sensors used eight cowl static-pressure taps, which resulted in nine output levels.

DESCRIPTION OF SENSOR

The continuous-output shock-position sensor is shown schematically in figure 6. The components and logic required for the continuous-output sensor are quite similar to those used in the stepwise-output sensor shown in figure 3. There are three additions to the circuit which made the sensor output continuous. A triangular wave was superimposed on each of the reference voltages by means of a triangular-wave generator. A

reference summing amplifier was added to each channel, and a filter was added to the output. The triangular-wave bias causes the reference voltage on each comparator to be a triangular wave whose midpoint was set a small amount higher than the supersonic value at each tap. The amplitude of the triangular wave was set at approximately 0.2 of the throat reference pressure. This value was selected during the wind-tunnel tests as a value that produced the most linear output signal as a function of inlet airflow. The frequency of the triangular wave was set at 1000 hertz.

When one of the wall static-pressure taps is within the range of the rapidly varying reference voltage, the output of the comparator of that tap will alternate between on and off. The length of time that the output will be on will depend on the magnitude of the pressure at that tap. The farther upstream the shock is, the longer the output of each comparator will remain on. The comparator will alternate between on and off at the same frequency as the reference voltage oscillation. The outputs of all the comparators are summed in the analog summing amplifier. The output of the summing amplifier is filtered to remove the high frequency (1000-Hz) component of the output. The output filter was a second-order filter with a natural frequency of 100 hertz and a damping ratio of 0.7. This frequency is well beyond the capability of the inlet control system and, therefore, will not affect the control-system performance.

EXPERIMENTAL TESTS

Apparatus

The terminal-shock-position sensor was tested in a YF-12 aircraft flight inlet. Tests were conducted in the Lewis 10- by 10-Foot Supersonic Wind Tunnel. (The apparatus is described in greater detail in ref. 8.)

Inlet. - Figure 7 is a cutaway view of the YF-12 aircraft inlet. It is a mixed-compression type inlet in which 60 percent of the supersonic area contraction occurs internally at the aircraft normal cruise Mach number. The spike is translated by a hydraulic actuator for inlet restart capability and off-design Mach-number operation. Spike boundary-layer control is provided by a slotted bleed surface (fig. 7). The bleed flow is taken out of the inlet through the spike support struts and is dumped overboard through louvered exits. A combination flush slot and ram scoop, that is referred to as the shock trap, controls the cowl boundary layer. The shock-trap flow combines with the aft-bypass flow and is exhausted through the engine ejector nozzle. The aft bypass system is used to aid the forward-bypass system in matching the inlet airflow to the engine airflow requirements at flight Mach numbers below 3. The forward-bypass system is used by the YF-12 aircraft inlet control system to regulate the terminal-shock position.

Pressure-instrumentation location. - The locations of the cowl static-pressure transducers used in the shock-position sensor are shown in figure 8. These transducer outputs were also used to evaluate the steady-state and dynamic performance of the sensor.

The pressure-tap measurements are made by close-coupled strain-gage type, high-response pressure transducers. The response of each transducer and its connecting line was flat to within 0 to ±0.5 decibel and had negligible phase shift in the frequency range of 0 to 100 hertz (the frequency range for which data are shown). Additional details of the transducers are given in reference 8. A fraction of the throat total pressure (at probe $P_{p,A}$) was used as a reference for the shock sensor and remained constant throughout frequency-response testing of the sensor.

Installation of inlet in wind tunnel. - A schematic diagram of the inlet installation in the wind tunnel is presented in figure 9. The inlet was attached to a boilerplate nacelle, and the entire assembly was mounted on a strut that extended through the tunnel ceiling. Inside the nacelle was a 3.05-meter long cold-pipe assembly.

When mounted on the aircraft, the spike longitudinal axis is canted downward 6.5° with respect to the engine axis, and the inlet is rotated 30° outboard to move the spike tip inboard. This is done to aline the inlet with the local flow field at normal cruise attitude. In the wind tunnel, the inlet was mounted upside down, with the plane of symmetry vertical. The transition section shown in figure 9 was inserted to keep the longitudinal axes of both the spike and cold pipe parallel to the tunnel flow. This arrangement resulted in maximum angle-of-attack variation. The inlet orientation in the tunnel is equivalent to that achieved by removing the cant between the spike and engine axes on the aircraft and rotating the engine top outboard 150° relative to the vertical plane. The orientation of the inlet in the tunnel relative to the orientation in the aircraft is shown in figure 9.

The assembly had a remotely controlled angle-of-attack capability of $\pm 6.4^{\circ}$ between the floor and ceiling boundary layers. The interface between the nacelle and the strut was designed to allow the angle of sideslip to be changed a maximum of $\pm 3^{\circ}$ between tunnel runs.

Airflow-disturbance generator. - During the inlet frequency-response testing, a specially designed airflow-disturbance generator was mounted on struts in the cold pipe. The assembly was installed at the upstream end of the cold pipe, near the compressor-face station, as shown schematically in figure 10. The assembly consisted of five sliding-plate valves, or disturbance doors, which were hinged so that they could be expanded and collapsed like an umbrella. Figure 11 shows the airflow-disturbance generator installed in the cold pipe and expanded about halfway. The hinged webs noted in figure 10 blocked the flow area between the doors. Flow across the assembly was choked. During the tunnel start procedure, the disturbance generator was collapsed completely out of the main-duct airstream to minimize tunnel blockage. The amount of expansion

required during a test was a function of the desired engine corrected airflow and was remotely controlled by an electrohydraulic servomechanism.

A single disturbance door is shown in figure 12. Each door had its own position servomechanism that was hydraulically actuated and electronically controlled. Position was measured by means of a linear variable differential transformer. Details of the disturbance door servomechanism design are given in reference 13. The disturbance-door position frequency response is shown in figure 13. The response shown is for disturbance amplitudes representative of those used in the inlet frequency-response tests - 10 to 20 percent of maximum door area.

Static Test Results

Steady-state performance tests were conducted on the terminal-shock-position sensor to determine the linearity of the sensor output with the actual shock position. The results of these tests for three angles of attack are plotted in figure 14. The tests were conducted by positioning the shock at several different locations in the duct by manually controlling the disturbance doors. At each location, readings were taken of shock-sensor output and the cowl static-pressure profile. The actual shock position was determined from the cowl static-pressure profile at each reading. Examples of cowl static-pressure profiles for three angles of attack are shown in figure 15. The actual shock position for each reading is determined by the intersection of the cowl static-pressure profile with the supersonic pressure profile. The supersonic profile, taken with the shock downstream of the pressure taps, is shown by the heavy line (rdg. 6).

The sensor output appears to be linear within ±5 percent of the total distance covered by the static-pressure-tap region (2 percent of the cowl radius). The maximum deviation of the output, caused by a change in angle of attack from 0° to 4°, is less than 25 percent of the total distance covered by the pressure-tap region (10 percent of the cowl radius). For the same 4° change in angle of attack, the gain of the sensor changes by 7 percent. In the region of the terminal-shock position during normal inlet operation (around tap $P_{s,A}$), the angle-of-attack error is negligible.

Dynamic Test Results

A test was also conducted to determine the frequency response of the shock sensor to terminal-shock motion. The shock motion was produced by sinusoidally oscillating all five airflow-disturbance doors. Figure 16 shows that shock position is quite linear with disturbance-door area.

The test was conducted at the following wind-tunnel and inlet conditions: free-stream Mach number, 2.955; free-stream temperature, 374 K; Reynolds number per meter, 3.99×10^6; inlet angle of attack and angle of sideslip, both 0°; forward- and aft-bypass door position, both closed; shock operating point, leading edge at tap $P_{s,F}$. The disturbance-door amplitude was adjusted until the shock displacement was about 12.5 centimeters on either side of the operating point. Disturbance-door position, shock-sensor output, and the outputs of the transducers connected to static taps $P_{s,A}$ to $P_{s,J}$ were recorded on magnetic tape for analysis.

It was desired to maintain a constant shock-position amplitude throughout the frequency-response test. Because the actual shock-position amplitude decreases with frequency when a constant disturbance-door amplitude is maintained, as shown in figure 17, it is necessary to increase the door amplitude at the higher frequencies. Because of physical limitations of the disturbance-door servosystem, a constant shock-position amplitude could be maintained only for frequencies below 40 hertz. A complete description of the method used to determine the actual shock position as a function of time from the cowl static pressures is given in reference 2.

Data analysis. - A time history of shock position at a given frequency can be determined from the recorded cowl static pressures. An example of these data is shown in figure 18. The frequency is 10 hertz. The sensor output and the pressures at taps $P_{s,A}$, $P_{s,B}$, $P_{s,D}$, $P_{s,F}$, $P_{s,G}$, and $P_{s,H}$ are shown. When the shock is downstream of a tap, the pressure at that tap is constant until the shock passes over the tap and moves upstream of it. The times at which the shock moved over tap $P_{s,A}$ while the shock was moving in the upstream and downstream directions are indicated in the figure. At each test frequency, the times of shock crossings and the positions of the taps were used to establish the actual shock position as a function of time. A digital computer program determined the best fit of the data to the equation $x_s = \Delta x \sin(\omega t + \varphi)$. In this equation, Δx is the zero-to-peak shock-motion amplitude, ω is the shock-motion frequency, and φ is the phase angle with respect to the time reference used in the computer program input data. The computer program was used also to determine the best fit of the sensor-output data to a similar equation. The phase shift between the sensor output and the actual shock position was then determined by subtracting the phase angles φ of the two equations, and the amplitude ratio was determined by dividing the sensor-output amplitude by the actual shock-position amplitude.

Test results. - Results of the frequency-response tests are shown in figure 19, where the data were normalized to their 1-hertz values. The normalized amplitude ratio was constant out to 60 hertz and dropped to 0.5 at about 100 hertz. The phase lag at this frequency is about 50°. A comparison of these results with the phase lag of the actual shock position to the disturbance-door motion (fig. 17) shows that at 100 hertz, the shock position lags the disturbance doors by about 620°. It can be concluded that for the YF-12

aircraft inlet, the phase lag of the shock-position sensor is negligible for control-system purposes.

SUMMARY OF RESULTS

This report describes the design and experimental performance of a new electronic terminal-shock-position sensor suitable for use with a mixed-compression inlet. The unique feature of this design is that the output signal is continuously proportional to the shock position. The outputs of referenced previous sensors were stepwise in nature, moving from one level to another as the shock moved within the inlet. The sensor determines shock position from the shape of the wall static-pressure profile as measured by 10 pressure taps in the cowl wall. Static tests demonstrated that the linearity of the sensor output was within ±5 percent of the total distance covered by the static-pressure-tap region (2 percent of the cowl radius). The maximum deviation of the output, caused by a change in the angle of attack from 0° to 4°, was less than 25 percent of the total distance covered by the pressure-tap region (10 percent of the cowl radius). For the same 4° change in the angle of attack, the gain of the sensor changed by 7 percent. In the region of the normal inlet operation, the angle-of-attack error was negligible.

Frequency-response tests on the sensor showed that the normalized amplitude decreases to 0.5 at about 100 hertz. The phase lag at 100 hertz was about 50°. When compared to the 620° that the shock position lags a compressor-face disturbance at 100 hertz, this 50° phase lag is almost negligible for control-system purposes.

Lewis Research Center,
National Aeronautics and Space Administration,
Cleveland, Ohio, February 12, 1974,
766-72.

REFERENCES

1. Campbell, David H.: F-12 Series Aircraft Propulsion System Performance and Development. Paper No. 73-821, AIAA, August 1973.

2. Griffin, William S.: Design and Performance of a Flueric Shock Position Sensor for a Mixed-Compression Supersonic Inlet. NASA TM X-1733, 1969.

3. Cole, Gary L.; Neiner, George H.; and Crosby, Michael J.: Design and Performance of a Digital Electronic Normal Shock Position Sensor for Mixed-Compression Inlets. NASA TN D-5606, 1969.

4. Dustin, Miles O.; Cole, Gary L.; and Wallhagen, Robert E.: Determination of Normal-Shock Position in a Mixed-Compression Supersonic Inlet. NASA TM X-2397, 1971.

5. Johnson, Elmer G.: Control Apparatus. Patent No. 3, 460, 554, United States, Aug. 1969.

6. Holmes, Allen B.; Gehman, Stacy E.; Egolf, David; and Lewellan, Michael: Flueric Normal Shock Sensor. Rep. TM-69-9, Harry Diamond Lab. (NASA CR-107688), Apr. 1969.

7. Dustin, Miles O.; and Cole, Gary L.: Performance Comparison of Three Normal-Shock Position Sensors for Mixed-Compression Inlets. NASA TM X-2739, 1973.

8. NASA Lewis Research Center: Wind-Tunnel Installation of Full-Scale Flight Inlet of YF-12 Aircraft for Steady-State and Dynamic Evaluation. NASA TM X-3138, 1974.

9. Neiner, George H.; Arpasi, Dale J.; and Dustin, Miles O.: Wind-Tunnel Evaluation of YF-12 Aircraft Inlet Control System by Frequency-Response and Transient Testing. NASA TM X-3142, 1974.

10. Neiner, George H.; Seidel, Robert C.; and Arpasi, Dale J.: Wind-Tunnel Evaluation of Experimental Controls on YF-12 Aircraft Flight Inlet by Frequency-Response and Transient Testing. NASA TM X-3143, 1974.

11. Cole, Gary L.; Cwynar, David S.; and Geyser, Lucille C.: Wind-Tunnel Evaluation of the Response of a YF-12 Aircraft Flight Inlet to Internal Airflow Perturbations by Frequency-Response Testing. NASA TM X-3141, 1974.

12. Cubbison, Robert W.: Wind-Tunnel Performance of an Isolated, Full-Scale, YF-12 Aircraft Inlet at Mach Numbers Above 2.1. NASA TM X-3139, 1974.

13. Webb, John A., Jr.; Mehmed, Oral; and Hiller, Kirby W.: Improved Design of a High-Response Slotted-Plate Overboard Bypass Valve for Supersonic Inlets. NASA TM X-2812, 1973.

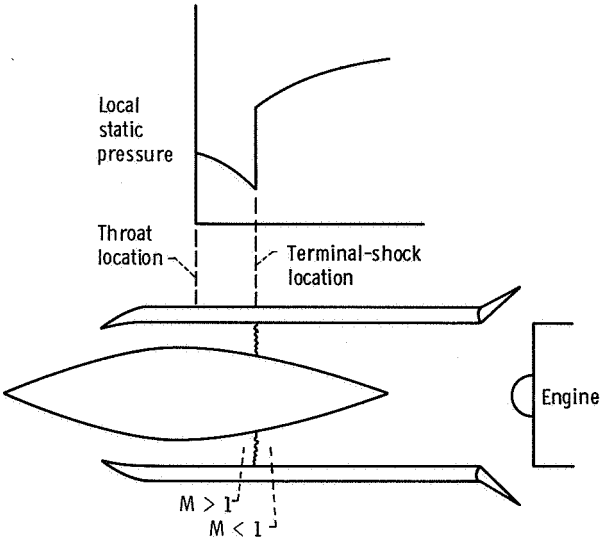

Figure 1. - Ideal static-pressure profile in vicinity of terminal shock.

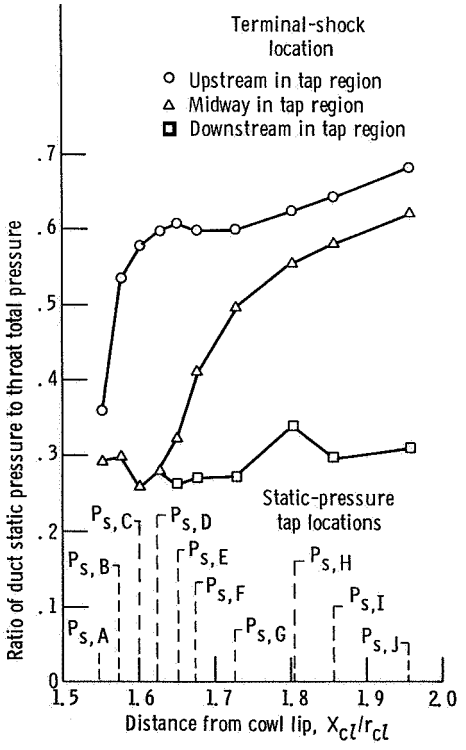

Figure 2. - Typical inlet cowl static-pressure profiles with terminal shock in three locations.

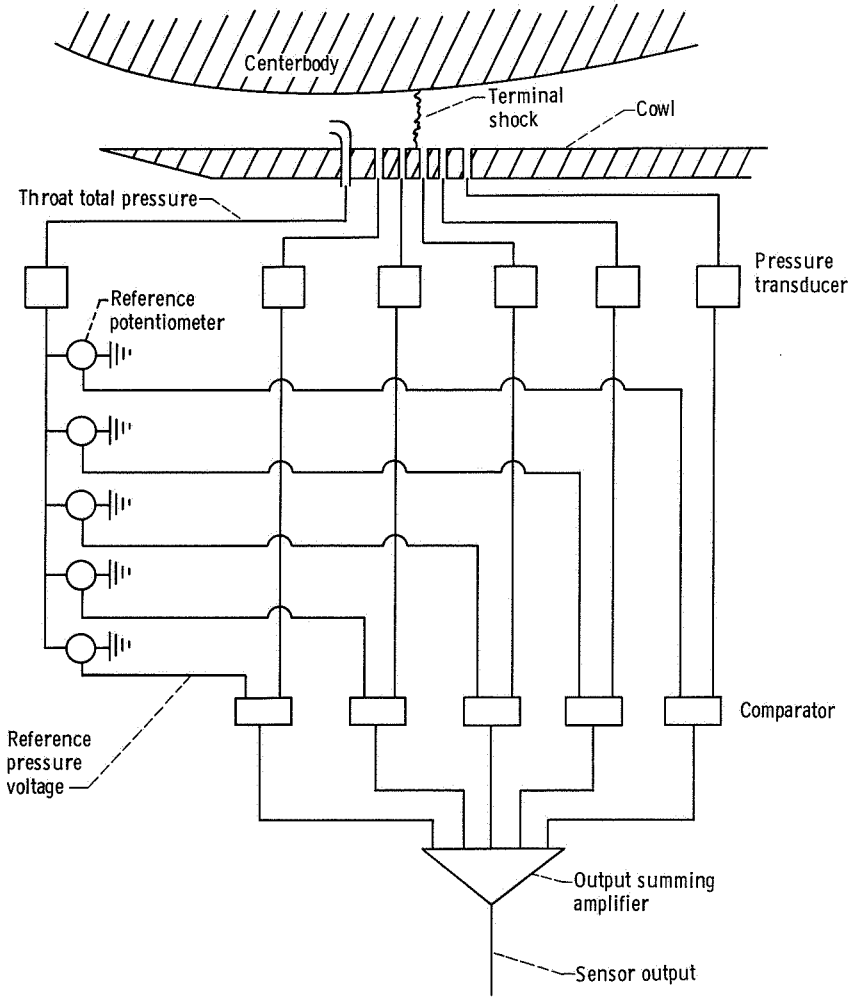

Figure 3. - Schematic diagram of stepwise-output shock-position sensor.

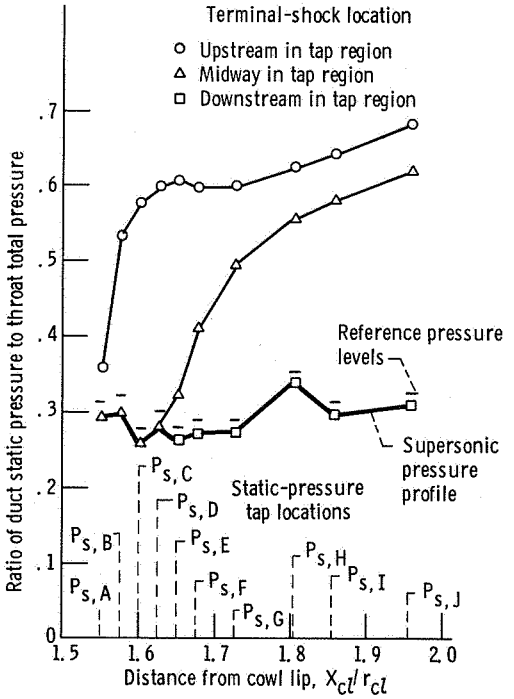

Figure 4. - Typical inlet cowl static-pressure profiles with terminal shock in three locations, with reference pressure levels shown.

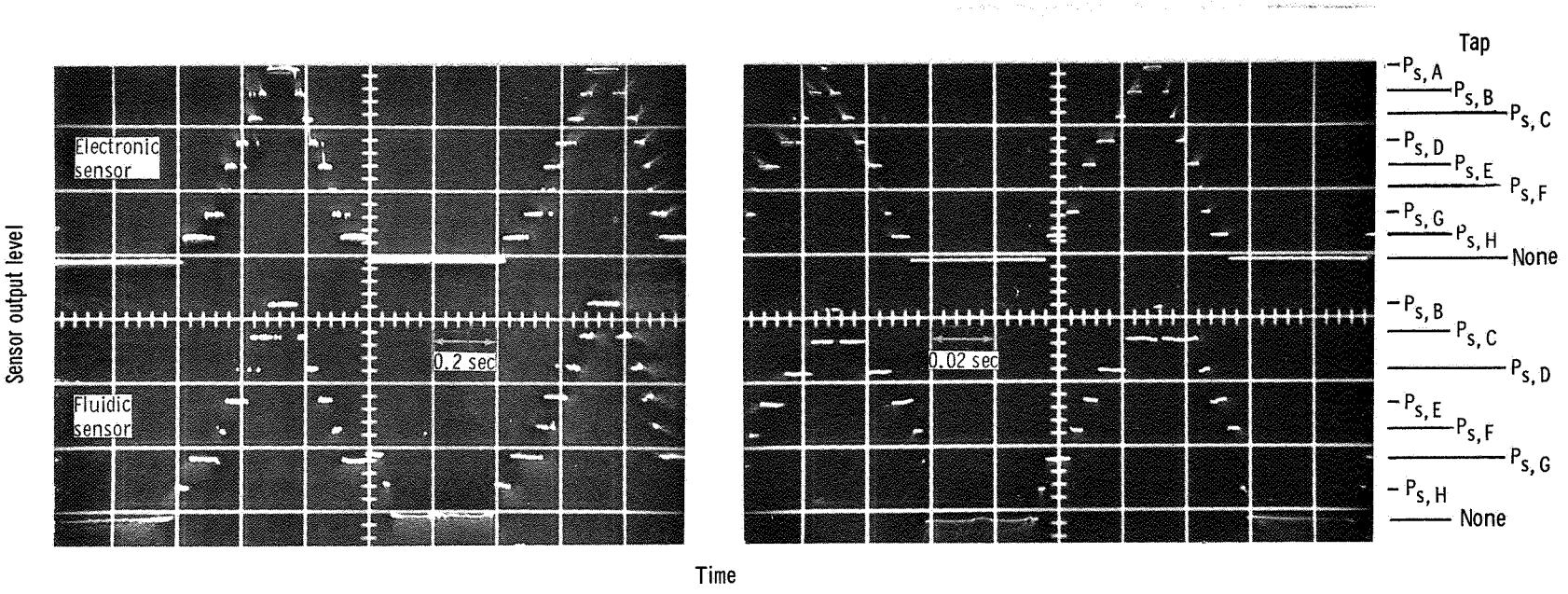

(a) Test frequency, 1 hertz.

(b) Test frequency, 10 hertz.

Figure 5. - Output responses of stepwise-output type shock-position sensors to sinusoidal engine-airflow disturbances. Each sensor had nine output levels. (From ref. 7.)

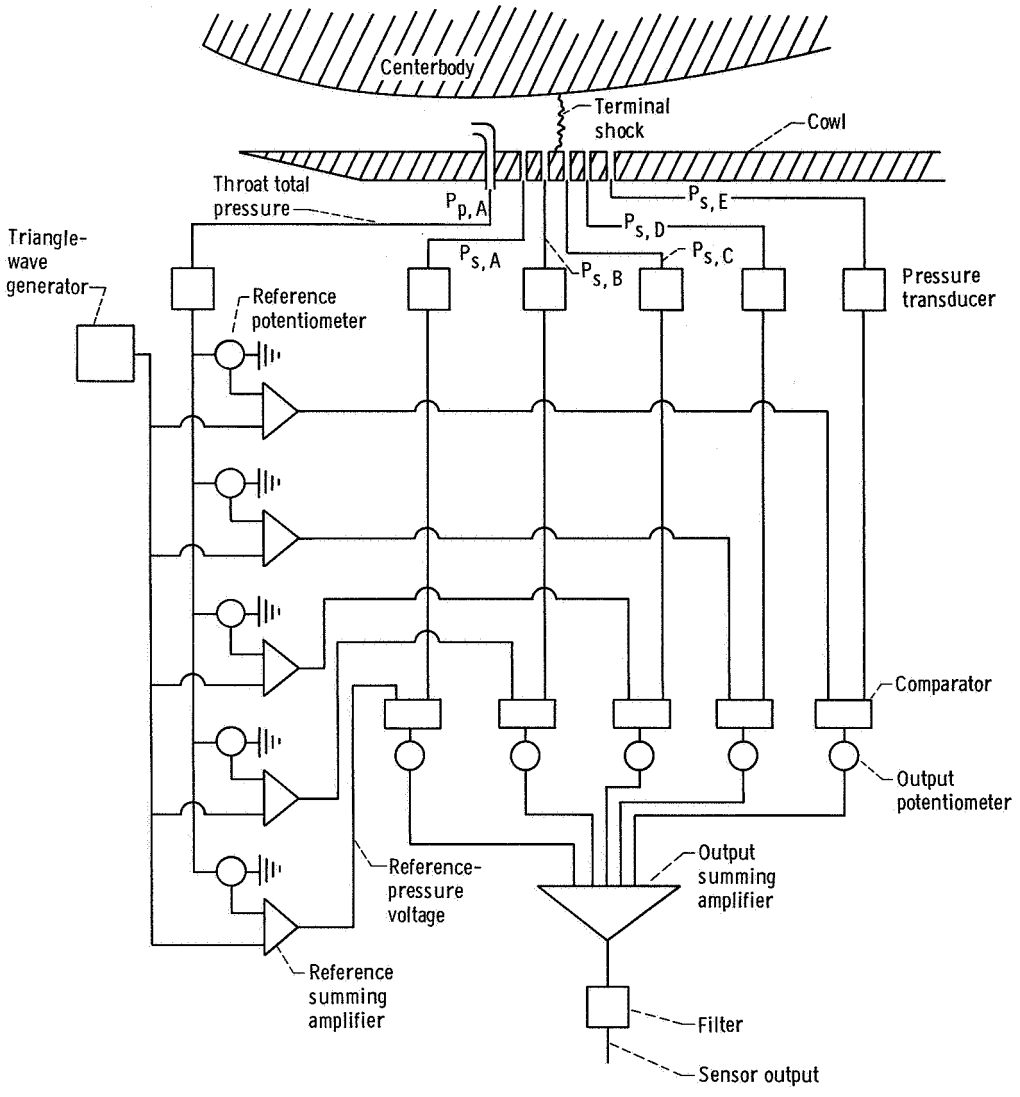

Figure 6. - Schematic diagram of continuous-output shock-position sensor.

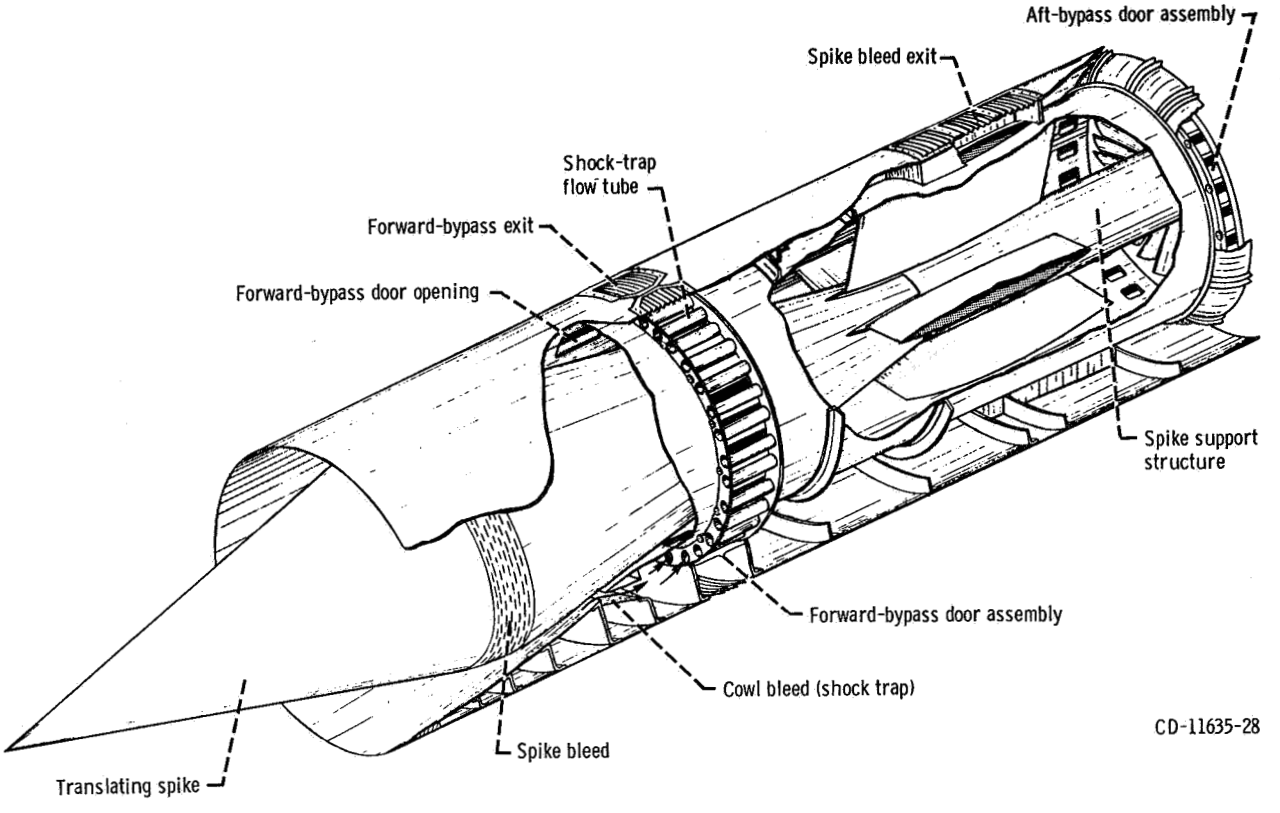

Figure 7. - Isometric view of flight inlet of YF-12 aircraft.

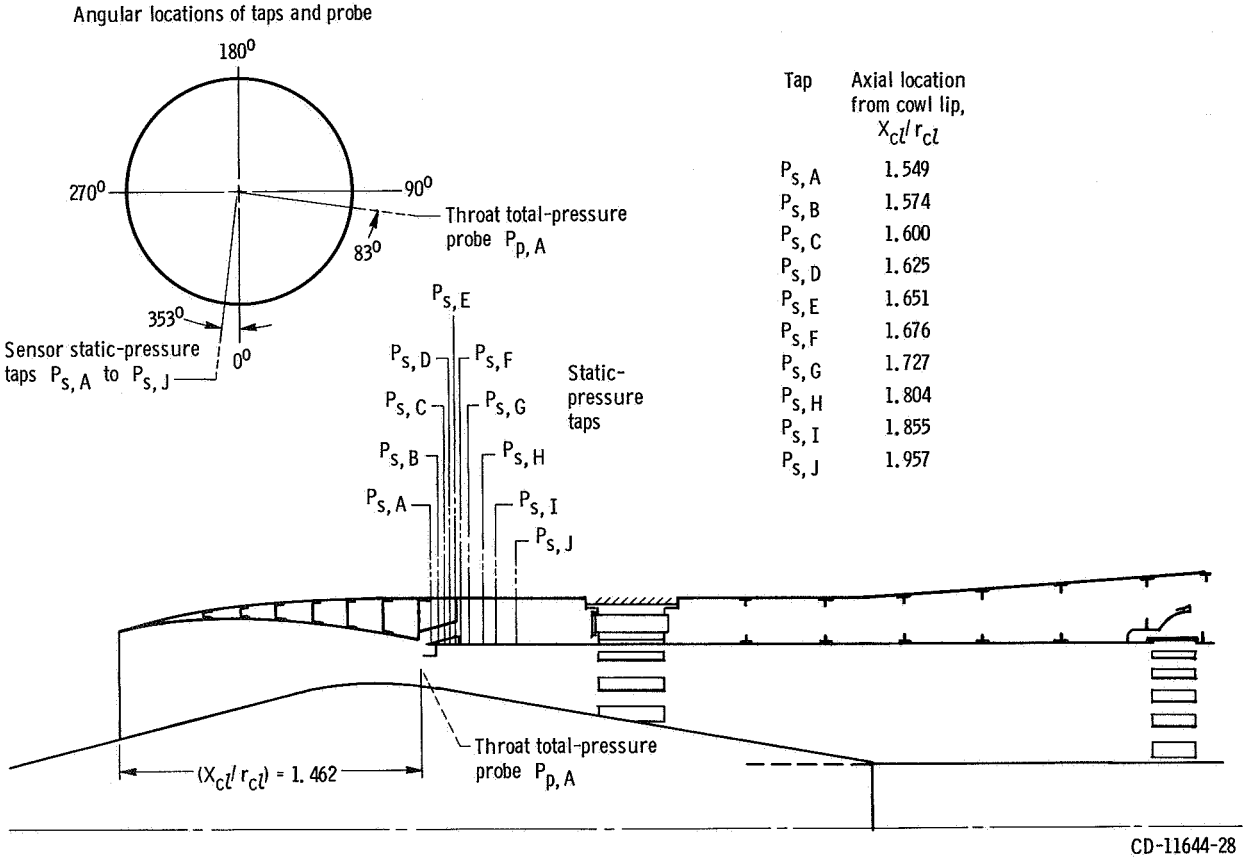

Figure 8. - Shock-sensor pressure-transducer locations. (Radius of cowl at cowl-lip station, r_{cl}, 74.62 cm.)

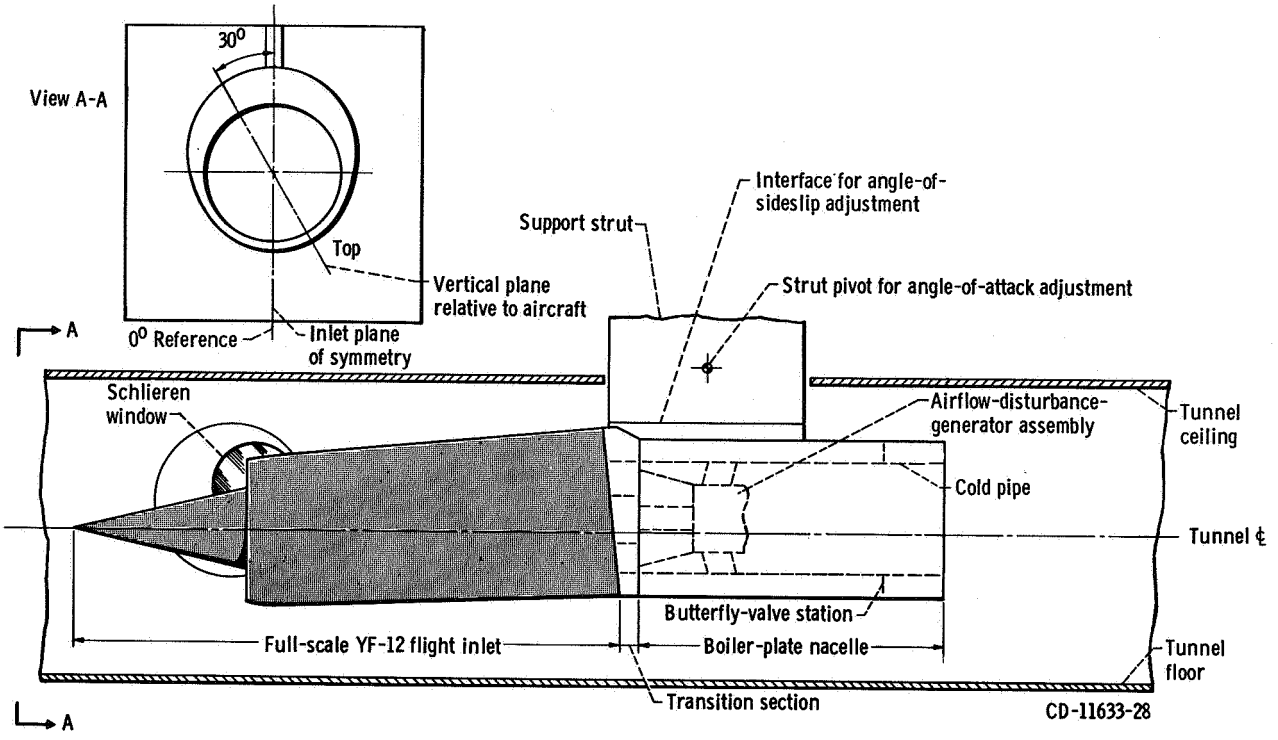

Figure 9. - Schematic diagram of inlet installation in test section of 10- by 10-Foot Supersonic Wind Tunnel.

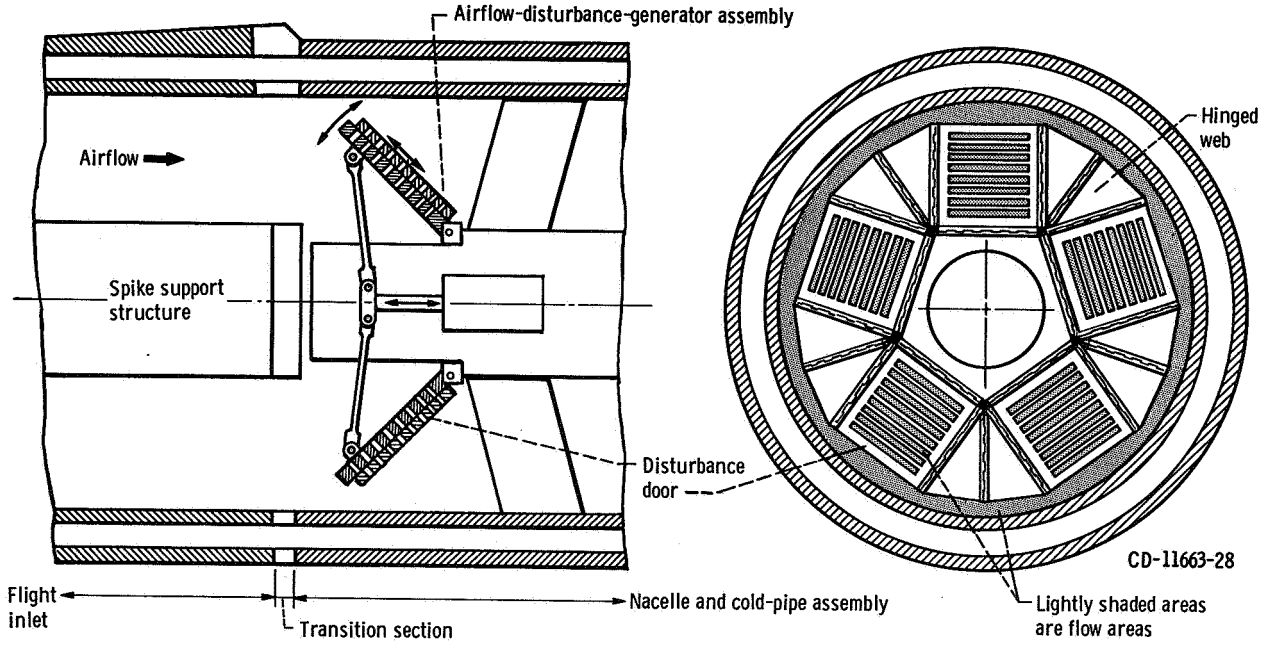

Figure 10. - Schematic diagram of airflow-disturbance generator.

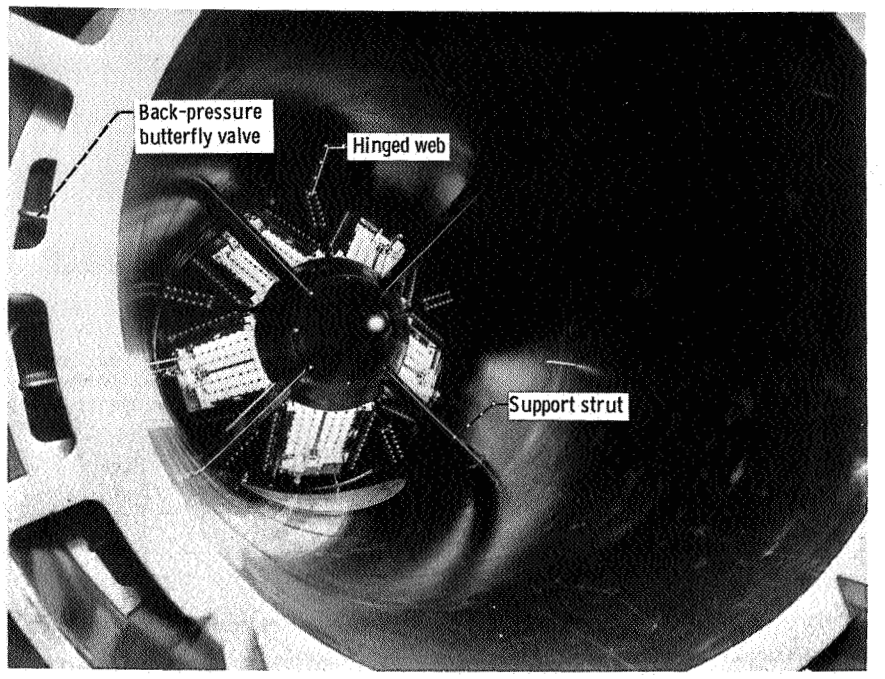

Figure 11. - Airflow-disturbance-generator assembly installed in cold pipe and expanded about halfway. (View looking upstream from aft end of cold pipe.)

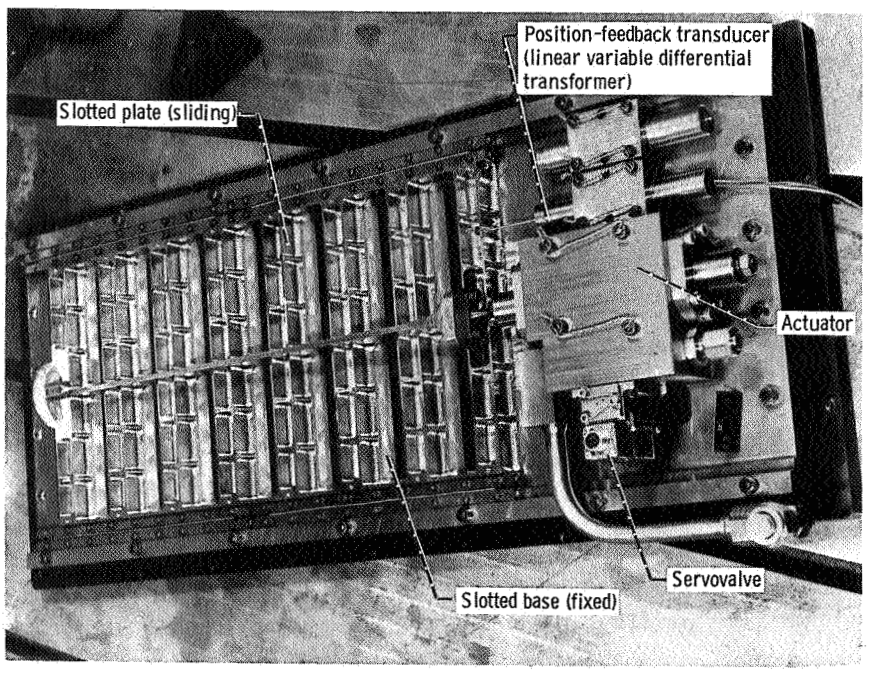

Figure 12. - Airflow-disturbance-generator sliding-plate valve (disturbance door).

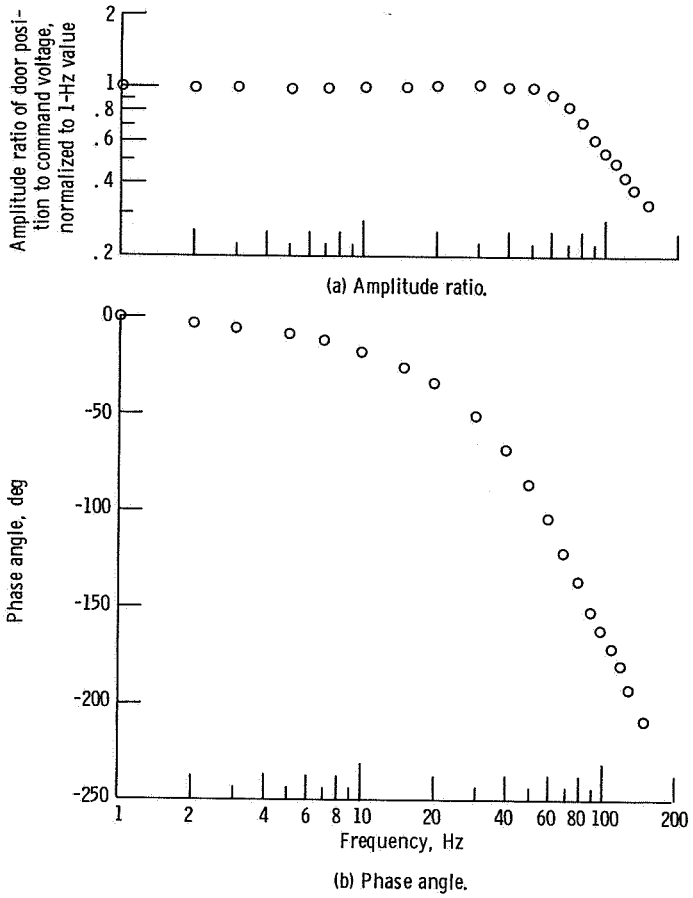

Figure 13. - Frequency response of position of sliding-plate valve (disturbance door) of airflow-disturbance generator to position command voltage. Commanded peak-to-peak amplitude represented an area change of 10 percent of maximum valve area.

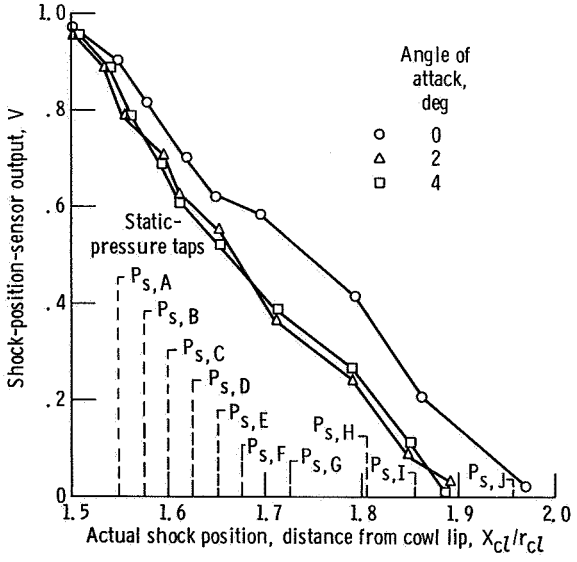

Figure 14. - Comparison of shock-sensor output with actual shock position. Mach number, 2.955; total temperature, 374 K.

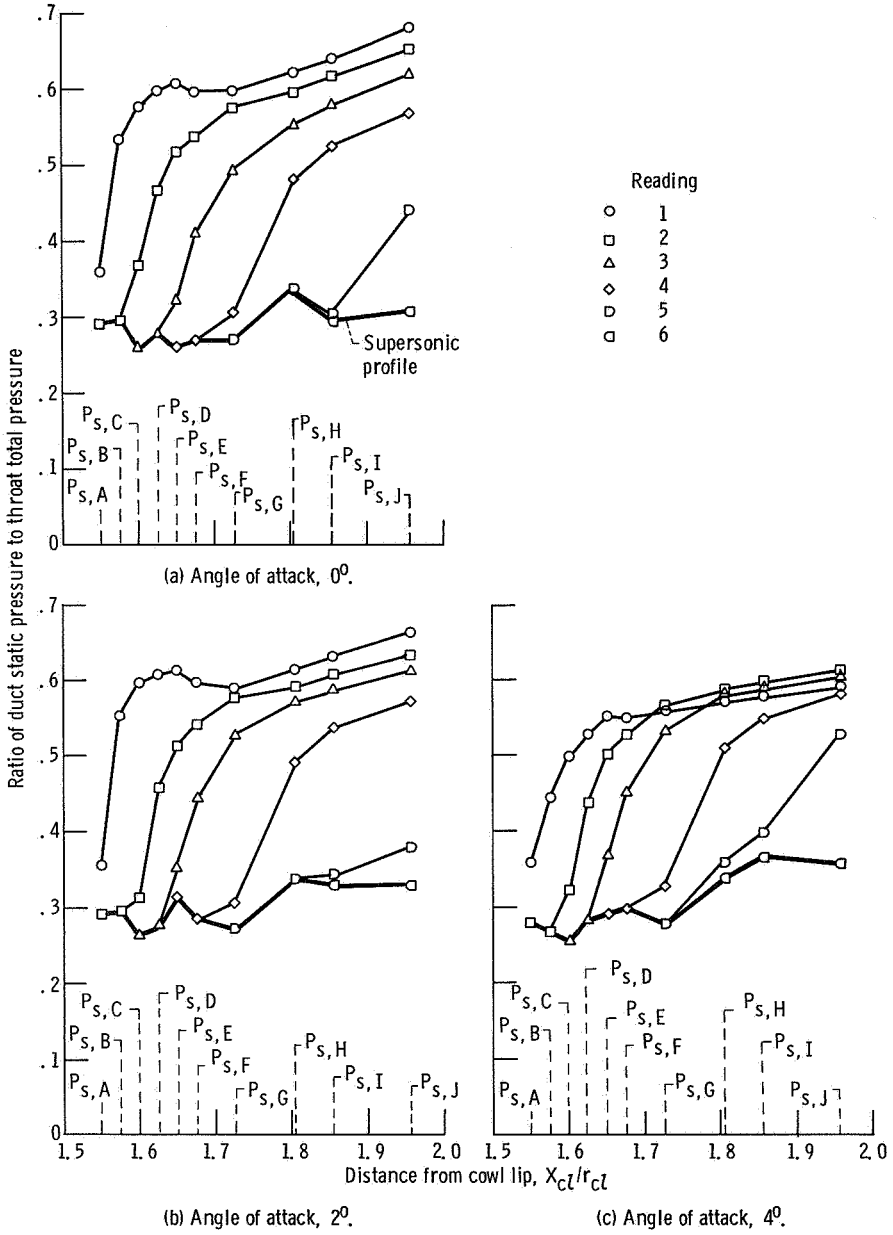

Figure 15. - Cowl static-pressure profiles for several shock positions. Mach number, 2.955; total temperature, 374 K.

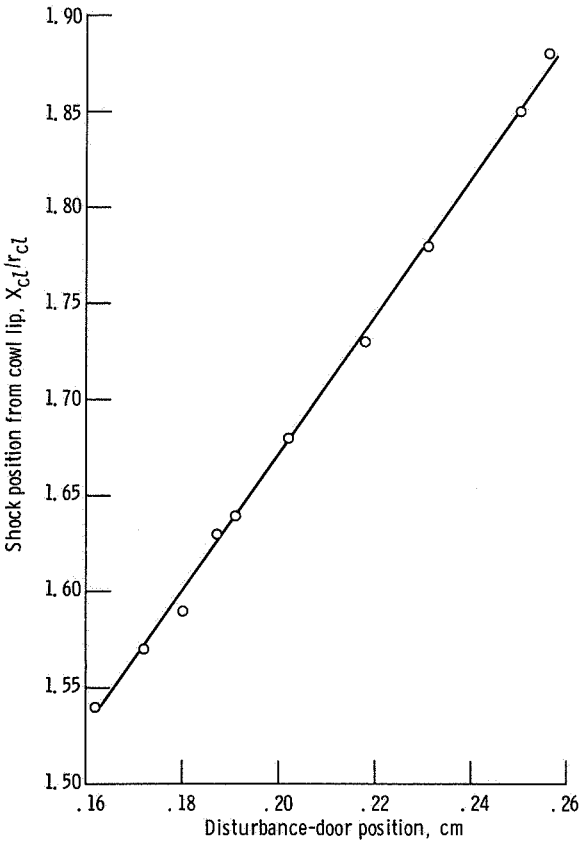

Figure 16. - Shock position as function of disturbance-door position.

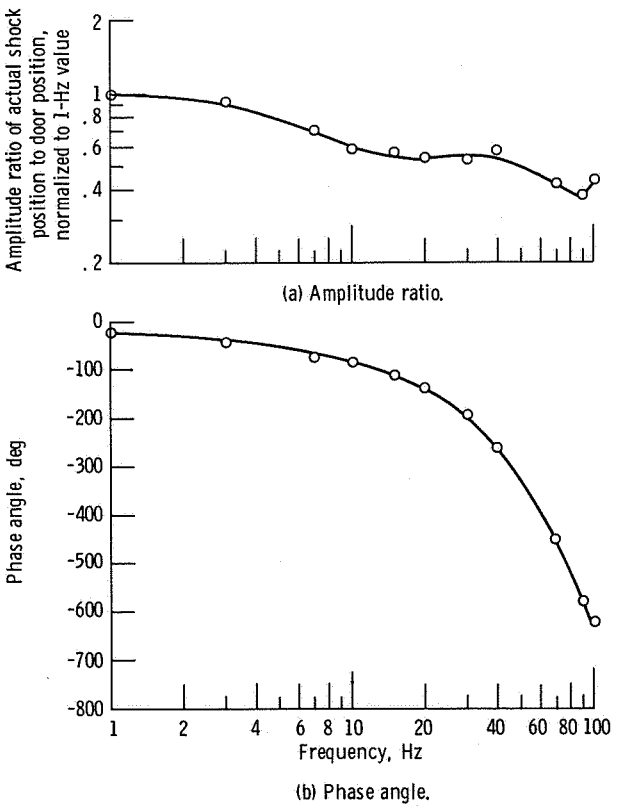

Figure 17. - Frequency response of actual shock position to disturbance-door position.

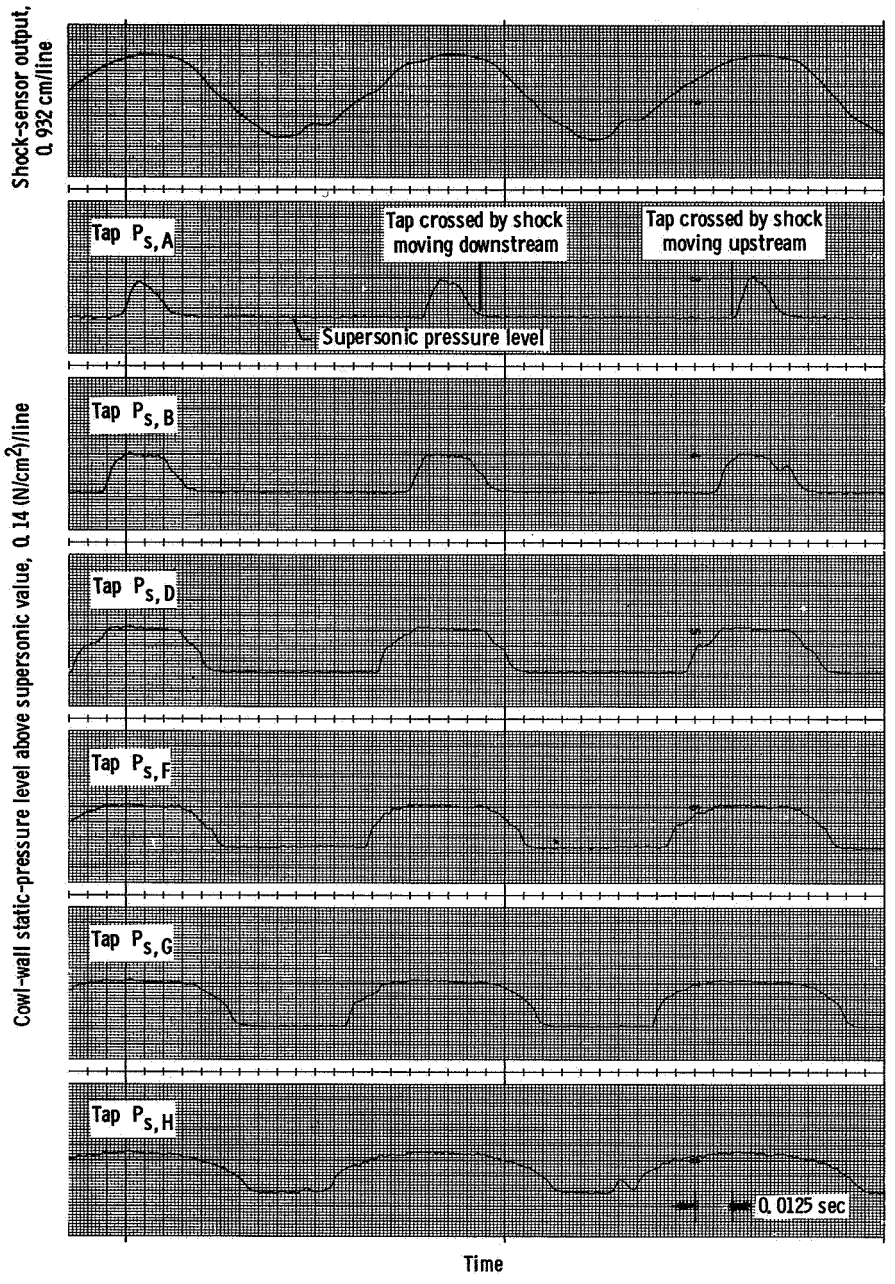

Figure 18. - Typical responses of cowl-wall static-pressure taps and shock-sensor output to sinusoidal changes in disturbance-door position. Frequency, 10 hertz.

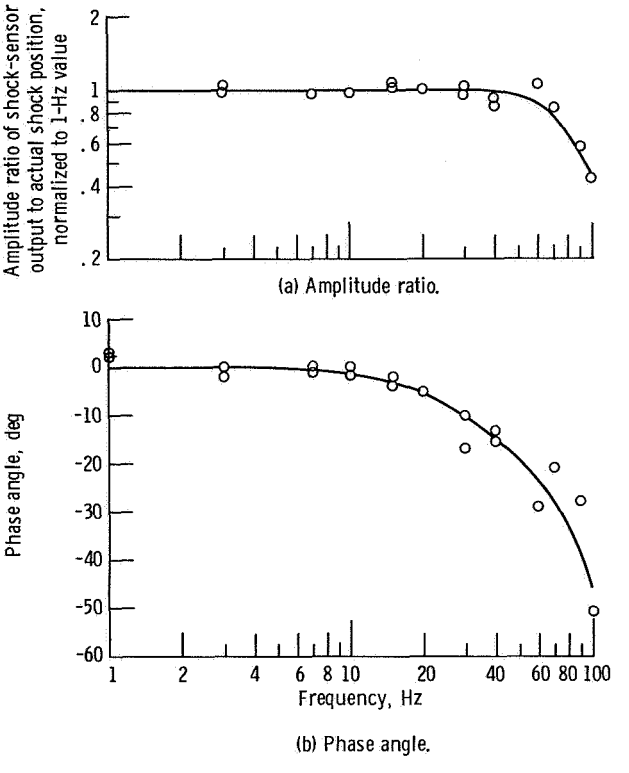

Figure 19. - Frequency response of terminal-shock-sensor output to actual shock position.

NATIONAL AERONAUTICS AND SPACE ADMINISTRATION
WASHINGTON, D.C. 20546

OFFICIAL BUSINESS
PENALTY FOR PRIVATE USE $300

SPECIAL FOURTH-CLASS RATE BOOK

POSTAGE AND FEES PAID
NATIONAL AERONAUTICS AND SPACE ADMINISTRATION
451

U.S. MAIL

POSTMASTER: If Undeliverable (Section 158 Postal Manual) Do Not Return

"The aeronautical and space activities of the United States shall be conducted so as to contribute . . . to the expansion of human knowledge of phenomena in the atmosphere and space. The Administration shall provide for the widest practicable and appropriate dissemination of information concerning its activities and the results thereof."

—NATIONAL AERONAUTICS AND SPACE ACT OF 1958

NASA SCIENTIFIC AND TECHNICAL PUBLICATIONS

TECHNICAL REPORTS: Scientific and technical information considered important, complete, and a lasting contribution to existing knowledge.

TECHNICAL NOTES: Information less broad in scope but nevertheless of importance as a contribution to existing knowledge.

TECHNICAL MEMORANDUMS: Information receiving limited distribution because of preliminary data, security classification, or other reasons. Also includes conference proceedings with either limited or unlimited distribution.

CONTRACTOR REPORTS: Scientific and technical information generated under a NASA contract or grant and considered an important contribution to existing knowledge.

TECHNICAL TRANSLATIONS: Information published in a foreign language considered to merit NASA distribution in English.

SPECIAL PUBLICATIONS: Information derived from or of value to NASA activities. Publications include final reports of major projects, monographs, data compilations, handbooks, sourcebooks, and special bibliographies.

TECHNOLOGY UTILIZATION PUBLICATIONS: Information on technology used by NASA that may be of particular interest in commercial and other non-aerospace applications. Publications include Tech Briefs, Technology Utilization Reports and Technology Surveys.

Details on the availability of these publications may be obtained from:

SCIENTIFIC AND TECHNICAL INFORMATION OFFICE

NATIONAL AERONAUTICS AND SPACE ADMINISTRATION

Washington, D.C. 20546